



PERGAMON

Computers & Graphics 23 (1999) 655–666

COMPUTERS
& GRAPHICS

www.elsevier.com/locate/cag

Visibility — techniques and applications

A qualitative and quantitative visibility analysis in urban scenes

Boaz Nadler*, Gadi Fibich, Shuly Lev-Yehudi, Daniel Cohen-Or

School of Mathematical Sciences, Tel Aviv University, Tel Aviv 69978, Israel

Abstract

In this paper we present a mathematical model of a generic urban scene, which can be used to answer a variety of visibility questions. Aside from its theoretical merit, the mathematical model provides an important analysis tool to optimize urban walkthrough algorithms. We formulate the probability for a given object to be visible from a given viewcell as a function of distance from the viewcell. We address various issues related to the implementation of virtual walkthrough, such as storage requirements, optimal viewcell size and cell-to-cell coherency, from which we derive space-effective data structures. Quantitative simulations verify the validity of our analysis. We simulate visibility in scenes with randomly distributed (Poisson) objects as well in pseudo-random (jittered) scenes, and compare these simulation results with our mathematical model. © 1999 Elsevier Science Ltd. All rights reserved.

Keywords: Visibility; Occlusion culling; Aspect graphs; Space subdivision; Probabilistic models

1. Introduction

Typical urban scenes are *densely occluded*, in the sense that from any given viewpoint only a small fraction of the scene is visible [1]. As a result, occlusion culling is vital for virtual walkthroughs in large urban scenes [1–4]. Most occlusion culling techniques are based on the assumption that for any given viewpoint there is a small set of objects which occludes most of the scene [3,5,6,13]. For example, nearby buildings are effective occluders in a typical urban scene [4]. The assumption that nearby objects cull the vast majority of remote objects seems to be intuitive when the density of the scene is high. However, in the case of sparser scenes the effectiveness of nearby objects decreases. This raises a variety of questions: What is the definition of ‘nearby’ objects and how does it depend on scene density? At what distance an object can be expected to be occluded? How many objects are visible from a given viewcell? The answers to these type of questions are less intuitive and require quantitative analysis based on a mathematical model.

In this paper we present a mathematical model of a generic urban scene which can be used to answer different visibility questions. Aside from its theoretical merit, the mathematical model provides an important analysis tool to optimize urban walkthrough algorithms. For example, given an urban scene with given density, one can quantitatively define the meaning of “close” versus “remote” regions. This quantitative definition is most important for walkthrough techniques which replace remote regions by simplified geometry or by *imposers* [7]. In other instances, based on our analysis, one can avoid rendering remote regions where the probability of missing significant objects is sufficiently low.

An important class of visibility problems concerns viewspace partitioning [1,8], in which visibility is computed for a small region or cell rather than for a point. It was shown that *cell visibility* is a vital tool for remote network-based walkthroughs [9]. In such applications clients are required to have a visibility cache, which the server updates with relevant cell visibility data. The server can either compute the cell visibility on-the-fly on demand, or precompute the cell visibility (or some of the cells) offline. In both cases, both server and client are required to maintain a data structure which stores the visibility sets of nearby cells. Implementation of this type of walkthrough raises various interesting problems. For

* Corresponding author.

E-mail address: nadlebo@math.tau.ac.il (B. Nadler)

example, since the visibility set of adjacent cells have many entities in common, storing the visibility set for each cell separately yields duplications of data. This implies that a good data structure can exploit this cell-to-cell visibility coherency by means of some difference lists or some hierarchical structure (e.g. a quadtree). Our mathematical model can estimate the size of the intersection of the visibility sets of adjacent cells or neighboring cells, as a function of scene density and cell size (Section 5). This estimate is necessary (i) to determine the optimal cell size and (ii) to design a space-effective data structure.

Generally speaking, exact visibility queries have a high computational complexity [10,11]. Several authors have developed approximate conservative visibility techniques, that is, techniques that compute a superset of the visibility set which includes all visible objects and perhaps some occluded objects. The advantage of such conservative sets is that they can be computed much faster than exact visibility sets [1,6]. The technique in [1] culls only objects for which there is a single (*strong*) occluder which by itself guarantees that the given object is not visible from any viewpoint within a viewcell. It was shown that for densely occluded scenes the majority of occluded objects are strongly occluded.

In this study, we analyze the visibility of objects in dense scenes by considering a two-dimensional space, filled with objects of the same size and shape. This is, of course, an approximation of an actual urban scene. However, it is a reasonable one for a flat scene with objects that are all about the same height and size, and for a viewer who is always located not higher than any of the objects. Nevertheless, since an urban scene is close to a 2.5D model, we also compute the visibility as a function of the object height with respect to the viewer (Section 3) and show that the addition of the heights has a relatively small effect on visibility probability.

Our mathematical model assumes that objects are uniformly randomly located over the entire scene, with constant density δ . In practice, this is not the general case, for two main reasons: (i) the density can vary between ‘neighborhoods’, and (ii) objects may not be randomly scattered, but rather located on a square grid with their locations randomly perturbed. The mathematical model can be extended for more general scenes, as we have illustrated in the extension to the 2.5D case. While this will result in more complex expressions, the main results of the model would remain unchanged: (i) the definition of ‘effective distance’ $d\delta/R$ and ‘effective viewcell size’ ϵ/R , (ii) the exponential decay of visibility and potential visibility with distance, (iii) the estimate (6), and (iv) the total number of visible objects is proportional to $1/\delta$. The advantage of our modeling approach is that it allows to classify visibility in real scenes as a function of a few parameters.

The paper is organized as follows. In Section 2 we define a mathematical model of an urban scene. In

Section 3 we analyze the visibility as a function of scene density and viewcell size. We give an explicit expression for the distance beyond which the probability of an object to be visible is less than a prescribed value. Section 4 is devoted to the estimation of visibility and potential-visibility set size, and to the analysis of the effectiveness of the potentially visible set. The cell-to-cell visibility coherency is analyzed in Section 5, and in Section 6 we develop a storage space analysis, and determine an optimal cell size (space wise). Derived from this storage analysis, we present a hierarchical data structure in Section 7 and we show some quantitative results of its implementation. In Section 8 we analyze the effect of the distribution function on the visibility, as an effort to model a more realistic urban scenario.

2. Mathematical model of visibility in urban scenes

We consider a two-dimensional scene consisting of a large number of equally sized circles (objects) with radius R , randomly distributed in the plane. The scene is also characterized by the parameter δ , which is the average area fraction covered by the objects:

$$\delta = n(A)\pi R^2/|A|,$$

where $|A|$ is the total area of the scene and $n(A)$ is the number of objects in A . We assume that the objects’ area density is constant throughout space, i.e., that for any sufficiently large region Ω (i.e. with area $|\Omega| \gg \pi R^2$), the expected value of $n(\Omega)$ is $\delta|\Omega|/\pi R^2$.

We consider a circular viewcell C_ϵ with radius ϵ ($\epsilon < R$) located somewhere in the scene. An object S is called *visible* if there is a straight line (ray of sight) which connects C_ϵ and S that does not intersect with any of the other objects. Following [1], we say that an object S is *strongly occluded* from viewcell C_ϵ if there exists an object T that completely occludes S from all viewpoints in C_ϵ . An object which is not strongly occluded is called *potentially-visible*. Fig. 1 shows a typical scene with a viewcell at the center.

3. The probability of visibility and potential visibility

In the calculations of the probabilities for an object S to be visible or potentially visible, we use the following standard result from probability theory (e.g. [12]):

Let us consider a two-dimensional scene A with equally-sized objects that are randomly uniformly distributed with average object density per unit area

$$\rho = \delta/\pi R^2 = n(A)/|A|.$$

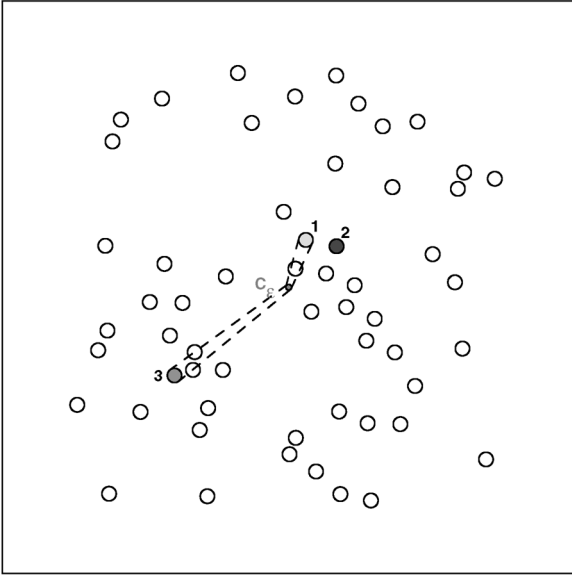


Fig. 1. Model representation of a typical flat urban scene. From the (red) viewcell C_ϵ , the green circle: (1) is strongly occluded, the blue circle, (2) is visible and the magenta circle, (3) is potentially visible (though not actually visible).

Then, the number of objects in a region $\Omega \subset A$ is approximately a Poisson distributed random variable with mean $\rho|\Omega|$, i.e.,

$$\Pr(n(\Omega) = k) \approx \exp(-\rho|\Omega|) \frac{(\rho|\Omega|)^k}{k!}, \quad k = 0, 1, \dots, \quad (1)$$

where $|\Omega|$ is the area of Ω and $n(\Omega)$ is the number of objects whose center is in Ω .

Eq. (1) is exact for $k = 0$. For $k > 0$, it is exact only when objects can overlap each other. However, relation (1) still serves as a good approximation for the distribution of $n(\Omega)$ in the case of non-overlapping objects when $|\Omega| \gg \pi R^2$ and $\delta \ll 1$.

In order to demonstrate the method which we use to calculate visibility probabilities, let us consider the following basic question. Given two point viewers located at a distance d apart, what is the probability that they see each other? As shown in Fig. 2, this happens only when there are no objects whose center resides inside the $d \times 2R$ rectangle. Therefore, according to (1) with $k = 0$,

$$\begin{aligned} \Pr(\text{viewers see each other}) &= \exp(-2\rho dR) \\ &= \exp\left(-\frac{2\delta d}{\pi R}\right). \end{aligned}$$

We now calculate the probability of potential visibility. Recall that an object is potentially visible if and only if it is not strongly occluded. To compute the probability of this event, we consider, without loss of generality, a viewcell C_ϵ centered at the origin and an object S centered at $(d, 0)$ (Fig. 3). We denote by Ω_S the ‘region of strong occlusion’ of the object S , which is defined as

$$\Omega_S = \{(x, y) \text{ an object } T \text{ centered at } (x, y) \text{ strongly occludes } S\}. \quad (2)$$

Obviously, an object S is potentially visible if and only if there are no objects whose center is inside Ω_S . For $d \gg R$ and $\epsilon < R$, the region Ω_S is approximately a triangle with height d and base $2(R - \epsilon)$. Therefore, using (1) with $k = 0$ gives

$$\begin{aligned} \Pr(S \text{ potentially visible}) &= \exp(-\delta|\Omega_S|/\pi R^2) \\ &\approx \exp\left(-\frac{1}{\pi} \frac{\delta d}{R} \left(1 - \frac{\epsilon}{R}\right)\right). \quad (3) \end{aligned}$$

Result (3) was derived for $\epsilon < R$. Indeed, when $\epsilon > R$ all objects are potentially visible, and relation (3) does not hold. The ‘discontinuity’ of potential visibility probability at $\epsilon = R$ will appear also in subsequent calculations.

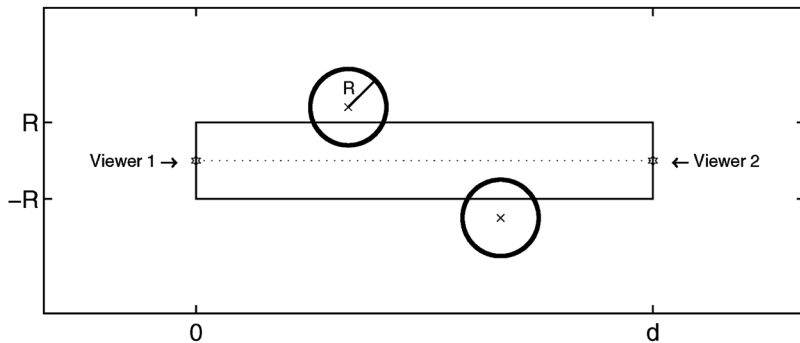


Fig. 2. Two viewers have eye contact if and only if the centers of all circles are outside the $d \times 2R$ rectangle.

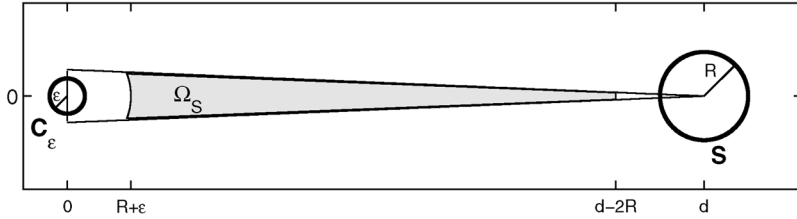


Fig. 3. The strong occlusion area Ω_S .

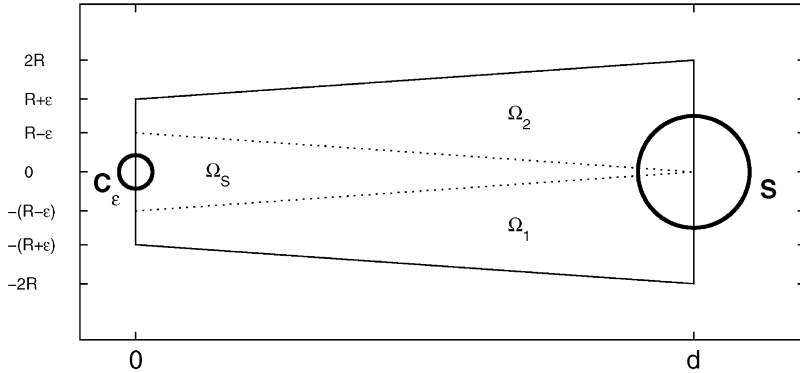


Fig. 4. The domain $\Omega = \Omega_S \cup \Omega_1 \cup \Omega_2$ (approximated for $d \gg R$).

To compute the probability that an object S is visible, we denote by Ω the ‘region of partial occlusion’ of S ,

$$\Omega = \{(x, y) \mid \text{an object } T \text{ centered at } (x, y) \text{ (partially) occludes } S\}. \tag{4}$$

In other words, an object whose center is inside Ω intersects with some rays connecting S and C_ϵ . When $d \gg R$, Ω is approximately given by a trapezoid with height d and bases $2R + 2\epsilon$ and $4R$ (Fig. 4).

The computation of the visibility probability was first done in [1], by replacing Ω with a rectangle with the same area and placing in this rectangle at random locations the expected number of objects inside Ω . Here, we perform a more accurate calculation, since we do not replace Ω with a rectangle, and we do not work with the expected number of objects inside Ω , but rather sum over all possible number of objects, multiplied by their respective probabilities.

The sketch of the calculation is as follows: We divide Ω into three disjoint regions Ω_S, Ω_1 and Ω_2 , where Ω_S is defined by Eq. (2), $\Omega_1 = (\Omega - \Omega_S) \cap \{y < 0\}$ and $\Omega_2 = (\Omega - \Omega_S) \cap \{y > 0\}$ (see Fig. 4). For S to be occluded, either Ω_S is not empty, or the bottom of the ‘lowest’ circle in Ω_2 is below¹ the top of the ‘highest’ circle in Ω_1 . Details

¹ Here we used the fact that $\epsilon < R$. In addition, we consider only horizontal rays of sight, which is a valid approximation when $d \gg R$.

of the calculations are presented in Appendix A, and their result is that

$$\Pr(S \text{ visible}) = \left[1 + \frac{\delta d}{\pi R} \left(1 + \frac{\epsilon}{R} \right) \right] \exp \left(- \frac{2}{\pi} \frac{\delta d}{R} \right). \tag{5}$$

The above calculation was done for the case of $\epsilon < R$, as in the calculation of potential visibility. However, unlike potential visibility, visibility does decrease exponentially with distance when $\epsilon > R$, albeit at a different rate than the one given in (5).

We note that a priori, visibility probabilities can be expected to depend on the four parameters δ, d, ϵ and R . However, our analysis shows that the visibility probabilities (3) and (5) depend only on *two* non-dimensional parameters: $\delta d/R$, and ϵ/R . In addition to reducing the dimension of the parameter space, we see that the definition of a ‘distant’ object depends not only on the distance itself, but rather on the non-dimensional parameter $\delta d/R$. Thus, an object is considered *far* from a visibility point of view when $\delta d/R \gg 1$. Furthermore, the effect of viewcell size on the visibility depends only on the ratio ϵ/R . This parameter plays an important role for potential visibility, as it affects the rate of the exponential decay.

Results (3) and (5) prove that *visibility and potentially visibility decay exponentially fast with distance*. Moreover, they provide the rate of decay, thus enabling a quantitative definition of a *far* object. For example, assuming that an object is defined as *far* when the probability that it is

visible is less than a prescribed threshold value p_{th} , then according to (5) all objects located at a distance

$$d > \frac{\pi R}{2\delta} \ln p_{th} \tag{6}$$

are far. Eq. (6) is important for techniques that replace far away objects by imposters or simplified geometry [7]. In addition, it can be used to control the expected error in cases one simply culls objects which are beyond a distance d .

As objects (houses) in a generic urban scene have different heights, we now consider the potential visibility in a 2.5D model. We assume that the viewcell is located on the ground at height zero, and that the height of all objects is uniformly distributed between h_1 and h_2 , ($h_1 < h_2$). We hence compute the probability that an object S with height h at a distance d is potentially visible from a viewcell of radius ϵ . In this case, the region Ω_S remains the same, but the density of occluding objects is not constant, and depends on the distance ξ from the viewcell:

$$\rho(\xi) = \begin{cases} \rho & \text{for } 0 < \xi < \frac{h_1}{h} d, \\ \rho \frac{h\xi/d - h_1}{h_2 - h_1} & \text{for } \frac{h_1}{h} d < \xi < d. \end{cases}$$

Therefore, instead of Eq. (3), the probability of potential visibility is now given by

$$\Pr(S \text{ potentially visible}) = \exp\left(-\int_{\Omega_S} \rho(y) dy\right).$$

Evaluation of the integral yields

$$\begin{aligned} \int_{\Omega_S} \rho(y) dy &= \int_0^d 2(R - \epsilon) \frac{d - \xi}{d} \rho(\xi) d\xi \\ &= \rho(R - \epsilon)d \left(1 - \frac{1}{3} \frac{(h - h_1)^3}{h^2(h_2 - h_1)}\right). \end{aligned}$$

Note that for $h = h_1$ we recover Eq. (3), since in this case height is irrelevant. As in the 2D case, visibility decays exponentially fast with distance but at a slower rate, since the ‘top’ of some buildings, whose ‘ground floor’ is occluded, can be seen.

To check the validity of the assumptions in our analysis (approximation of Ω_S by triangle, overlapping assumption, horizontal line of sight, etc.), we perform the following simulation. A large number of circles are randomly distributed in a square scene, and both visibility and potential visibility of all objects with respect to a viewcell at the scene’s center are computed. The results are averaged over 100 simulations with different randomly chosen object’s locations. As seen in Fig. 5, up to a statistical error, the averaged simulation results are in very good agreement with those predicted by the mathematical model (Eqs. (3) and (5)). Note that for exact visibility, prediction (5) is an underestimate for closer objects, due to the horizontal lines of sight approximation. However, at large distances, the horizontal lines approximation is valid, but due to the Poisson approximation where circles can overlap, Eq. (5) is an overestimate of the exact visibility.

4. The visibility set size

We now estimate N_{visible} and $N_{\text{potentially visible}}$, the average number of visible and potentially visible objects seen from a viewcell, respectively. We calculate these estimates by multiplying the expected number of objects at distances between r and $r + dr$ from viewcell by the probability that they are visible or potentially visible, and integrating over all rings. Since (3) and (5) are calculated under the assumption that $d \gg R$, we choose an arbitrary radius $r_0 = \alpha R$ and assume that all objects at distance less than r_0 are visible. Using (5), the average number of visible objects is therefore bounded by

$$N_{\text{visible}} \approx \pi r_0^2 \frac{\delta}{\pi R^2}$$

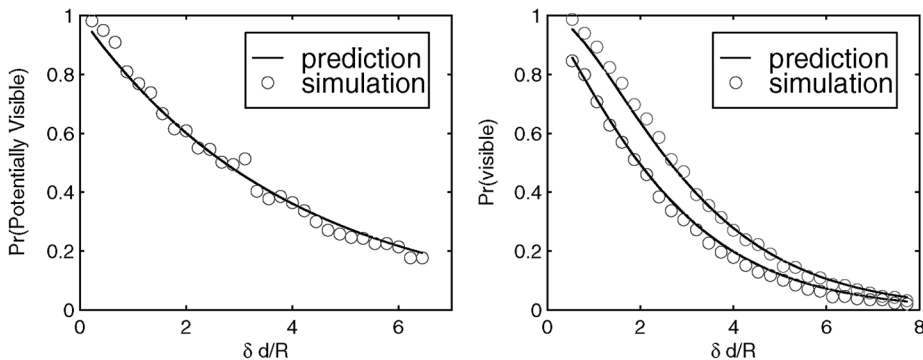


Fig. 5. Probability of visibility and potential visibility as function of non-dimensional distance $\delta d/R$, for a scene with $\delta = 0.1$, and $R = 1$. On the left, comparison of theoretical prediction, Eq. (3) with average of 100 simulations, for a viewcell size $\epsilon = 0.2R$. On the right, comparison of Eq. (5) with simulations for two different viewcell sizes: $\epsilon = 0.2R$ (bottom) and $\epsilon = R$ (top).

$$\begin{aligned}
 & + \int_{r_0}^{\infty} \Pr(S \text{ visible at distance } r) \frac{\delta}{\pi R^2} 2\pi r \, dr \\
 = & \delta \alpha^2 + \left[\left(\frac{\pi^2}{\delta} + 2\pi\alpha \right) \left(1 + \frac{\epsilon}{2R} \right) \right. \\
 & \left. + 2\delta \alpha^2 \left(1 + \frac{\epsilon}{R} \right) \right] \exp\left(\frac{-2\delta}{\pi} \alpha \right).
 \end{aligned}$$

Similarly, the average number of potentially visible objects is given by

$$\begin{aligned}
 N_{\text{potentially visible}} = & \delta \alpha^2 + 2\pi \left[\frac{\alpha}{(1 - \epsilon/R)} + \frac{1}{(1 - \epsilon/R)^2} \frac{\pi}{\delta} \right] \\
 & \times \exp\left(-\frac{\delta \alpha}{\pi} \left(1 - \frac{\epsilon}{R} \right) \right).
 \end{aligned}$$

Note that both N_{visible} and $N_{\text{potentially visible}}$ depend on δ only through the combination $\delta\alpha/\pi$ which is a small number. Therefore, we can set $\alpha = 0$, to obtain simpler expressions:

$$N_{\text{visible}} \approx \frac{\pi^2}{\delta} \left(1 + \frac{\epsilon}{2R} \right), \tag{7}$$

$$N_{\text{potentially visible}} \approx \frac{2\pi^2}{\delta} \frac{1}{(1 - \epsilon/R)^2}. \tag{8}$$

These results agree with intuition that the number of visible and potentially visible objects is monotonically decreasing with δ . However, our analysis shows that the number of visible and potentially visible objects is proportional to $1/\delta$, and not, for example, to $1/\sqrt{\delta}$. Note that these estimates are computed for circular viewcells. As shown in Appendix B, these results hold also for a square viewcell with side 2ϵ , albeit with an ‘effective’ diameter which is approximately 1.27 ϵ .

An important issue in implementation of potential-visibility-based algorithms is how much larger is the superset of potentially visible objects than the exact visibility set. To address this issue, we first note that from (3) and (5) we have that

$\Pr(\text{object strongly occluded} | \text{object not visible})$

$$\approx \frac{1 - \exp(- (1/\pi)(\delta d/R)(1 - (\epsilon/R)))}{1 - (1 + (\delta d/\pi R)(1 + \epsilon/R)) \exp(- (2/\pi)\delta d/R)}.$$

Therefore, most distant objects (with $\delta d/R \gg 1$) which are not visible are indeed strongly occluded. On the other hand,

$\Pr(\text{object visible} | \text{object potentially visible})$

$$\approx \frac{\exp(- (2/\pi)\delta d/R)}{(1 + (\delta d/\pi R)(1 + \epsilon/R)) \exp(- (1/\pi)(\delta d/R)(1 - \epsilon/R))},$$

which means that few of the distant objects which are potentially visible are actually visible. However, since the number of distant potentially visible objects is exponentially small, the potential visibility set is not much larger than the exact visibility set. Indeed, using (7) and (8) we can estimate that

$$\frac{N_{\text{potentially visible}}}{N_{\text{visible}}} \approx 2 \frac{(1 + \epsilon/2R)}{(1 - \epsilon/R)^2}. \tag{9}$$

Therefore, to avoid a large overhead when working with the strong occluders, the ratio ϵ/R (viewcell size/object size) should be sufficiently small. However, regardless of how small C_ϵ is, the overhead is no less than 2.

To check estimates (7) and (8) for N_{visible} and $N_{\text{potentially visible}}$ respectively, in the simulation described earlier we compute the number of potentially visible objects seen from a viewcell, both as a function of scene density (with constant viewcell size), and as a function of viewcell size (with constant density). The averaged results of 100 simulations are shown in Figs. 6 and 7. As expected, better agreement can be seen for smaller δ and ϵ/R . The simulation results are slightly lower than those predicted by the model, due to the finite size of the simulation scene, and due to the approximations made in the derivation of the theoretical estimates (7) and (8). Nevertheless, the simulation results confirm the predictions of the mathematical model that (1) size of visibility sets are proportional to $1/\delta$, and (2) N_{visible}

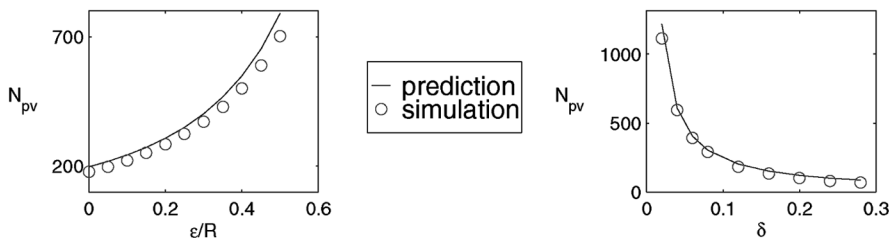


Fig. 6. Number of potentially visible objects as a function of non-dimensional viewcell size, ϵ/R , (left) with $\delta = 0.1$, and as a function of density (right) with $\epsilon/R = 0.1$. Comparison of theoretical prediction, Eq. (8) with average of 100 simulations.

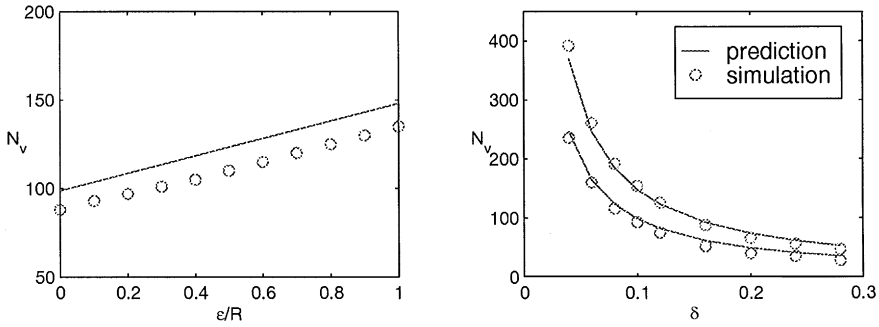


Fig. 7. Number of visible objects as a function of viewcell size (left) with $\delta = 0.1$, and as a function of density (right) with $\epsilon = 0.2R$ (bottom) and $\epsilon = R$ (top). Comparison of theoretical prediction, Eq. (7) with average of 100 simulations.

increases linearly with (non-dimensional) viewcell size ϵ/R .

5. Cell-to-cell-coherency

As stated in the introduction, the visibility set of nearby cells and especially of adjacent cells, have many entities in common. In this section, we estimate the intersection of the visibility sets of adjacent cells. This important quantity is needed to develop efficient data structures for an interactive walkthrough system.

Consider two tangentially adjacent circular viewcells C_ϵ^1 and C_ϵ^2 , and let Q_1 and Q_2 denote their corresponding potential visibility sets. We hence estimate the size of their intersection set $Q_1 \cap Q_2$, for $\epsilon/R < 1/2$. To this end, we consider an object S located at a distance d from the first viewcell. Let Ω_1 and Ω_2 denote the strong occlusion regions of S with respect to the two viewcells, respectively. The object S is potentially visible from *both* viewcells if and only if there are no objects whose center reside inside $\Omega_1 \cup \Omega_2$. Therefore,

Pr (S potentially visible from both viewcells)

$$\sim \exp\left(-\frac{\delta}{\pi R^2} |\Omega_1 \cup \Omega_2|\right).$$

The area of $\Omega_1 \cup \Omega_2$ depends on the angle θ between

the line connecting the first viewcell and the object, and the line connecting the two viewcells. To simplify the presentation, instead of computing the exact area of this region as a function of θ , we bound it by its upper value, which is attained at $\theta = \pi/2$, as shown in Fig. 8. For $d \gg R$ and $\theta = \pi/2$, $\Omega_1 \cup \Omega_2$ is approximately a triangle with height d and base $2R$. Therefore, for all values of θ ,

$$|\Omega_1 \cup \Omega_2| \leq Rd.$$

We now estimate $|Q_1 \cap Q_2|$, the average number of objects potentially visible from both viewcells. Using similar computations to those of Section 4, we obtain that

$$|Q_1 \cap Q_2| \approx \int_0^\infty 2\pi r \frac{\delta}{\pi R^2} \exp\left(-\frac{\delta r}{\pi R}\right) dr = \frac{2\pi^2}{\delta}.$$

Therefore,

$$\frac{|Q_1 \cap Q_2|}{|Q_1|} \approx \left(1 - \frac{\epsilon}{R}\right)^2.$$

We thus see that the relative overlap of the two adjacent visibility sets decreases *linearly* with viewcell size and that there is a high cell-to-cell coherency for small viewcells. For example, for $\epsilon/R = 0.1$ the overlap is about 80% of the size of the original sets. Further research is needed, to develop efficient data structures that exploit

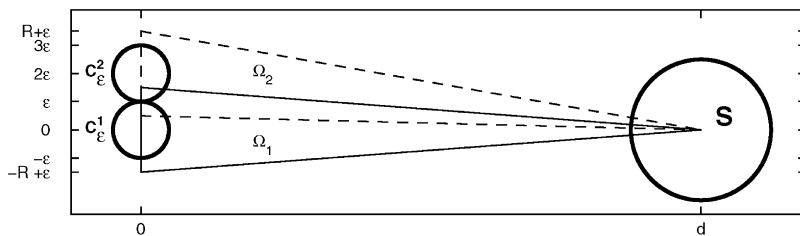


Fig. 8. Regions of strong occlusion for adjacent viewcells with $\theta = \pi/2$, for $d \gg R$.

this feature. Possible data structures are either difference lists or some hierarchical structure (e.g. a quadtree), where the links between nodes encode the difference sets.

6. Storage considerations

The analysis in Section 4 shows that for the strong occlusion approach to be effective, the viewcell has to be sufficiently smaller than the objects. However, there is no point in taking extremely small viewcells, since even as ϵ tends to zero the number of potentially visible objects cannot go below $2\pi^2/\delta$, which is the number of potentially visible objects from the viewcell center point (8). In addition, partitioning the scene into smaller viewcells increases the number of viewcells, which is highly undesirable, especially if we precompute and store each viewcell's potential visibility set. Thus, the following question arises: What is the optimal way to partition a scene into viewcells?

We can answer this question from the point of view of minimizing the overall storage, assuming that for each viewcell we store all of its corresponding potential visibility set. For example, if we partition an M by M scene into N^2 viewcells, each with sides $2\epsilon = M/N$, the total storage required is given by

$$G(\epsilon) \approx \frac{M^2}{4\epsilon^2} N_{\text{potentially visible}}(\epsilon).$$

The optimal viewcell size can be found from $G'(\epsilon) = 0$. Since $N_{\text{potentially visible}}$ for a square viewcell can be approximated using (B.1), the optimal value of ϵ/R is $1/(1.27 \times 2\sqrt{2}) \approx 0.3$. For a real scene, this procedure can be repeated, only with $N_{\text{potentially visible}}(\epsilon)$ computed directly from simulations.

7. Hierarchical data structure

As we have already said, one approach for reducing rendering time in interactive walkthrough systems is to compute the visibility set for a square viewcell, rather than for a certain view-point. Thus, the purpose becomes to compute the set of polygons (or objects) which are potentially visible from every point within the cell, from the set of polygons of the entire scene. One way to achieve a reasonable latency time is to pre-compute the visibility sets of all cells in the environment, and during the walkthrough fetch the appropriate list and render it. However, since the change in visibility from adjacent cells is usually small, their lists include many common objects. As a result, there are many duplications of polygons (objects) in the data structure. For a typical scene, consisting of hundreds of thousands of polygons, the amount of produced data is too large.

We can exploit the cell-to-cell coherency, predicted by the model (Section 5), to store the data in a hierarchical data structure which reduces the number of duplications. To this end, we divide the scene into 'large' $4\epsilon \times 4\epsilon$ squares, each consisting of four adjacent viewcells with sides 2ϵ . For each of the four adjacent cells we compute its potential-visibility set T_i ($i = 1,2,3,4$) and the intersection set $T_{1234} = \cap_{i=1}^4 T_i$. In the data structure, for each 'large' square, we store the intersection set T_{1234} and the four difference lists ($T_i - T_{1234}$). Thus, the rendering list of cell i consists of the two (disjoint) lists T_{1234} and $(T_i - T_{1234})$.

To evaluate the effectiveness of the proposed data structure, we implement a simulation program with two scenes, each consisting of randomly distributed identical square objects (with side $2R = 40$). The first scene includes 4500 objects (9000 polygons) in an environment with density $\delta = 0.2$. The second scene includes 5062 objects (10124 polygons) with density $\delta = 0.09$. We place four adjacent square viewcells at the center of the scene and compute the corresponding sets T_i ($i = 1,2,3,4$) and T_{1234} .

Fig. 9(a) shows the average coherence ratio $4|T_{1234}|/\sum_{i=1}^4|T_i|$, as a function of cell size for the first scene ($\delta = 0.2$). As expected, coherence approaches its maximum (= 100%) when either ϵ/R goes to zero or when ϵ becomes comparable to R and all objects become potentially visible.

In Fig. 9(b) we plot the total storage size of the naive data-structure ($M^2\sum_{i=1}^4|T_i(\epsilon)|/16\epsilon^2$) and of the hierarchical data structure ($M^2(\sum_{i=1}^4|T_i(\epsilon)| - 3|T_{1234}|)/16\epsilon^2$), as a function of cell size for the second scene ($\delta = 0.09$). In these simulations the use of the hierarchical data-structure leads to savings in total storage of about 25%. The optimal cell size for the naive data-structure is $\epsilon/R \approx 0.5$, which is close to the analytic prediction (Section 6). The optimal cell size for the hierarchical data-structure is slightly lower.

8. Visibility in jittered scenes – simulation analysis

In our analysis so far, we assumed that objects are randomly distributed inside the scene. Clearly, this is not the case for urban scenes, where houses are not randomly scattered, but rather jittered with respect to some underlying structure (grid, topography, etc.). In order to see how this affects visibility, we consider a scene with an underlying grid structure. The scene is divided into equally sized squares (lots) with side L , such that each square contains exactly one circle of radius R . The center of the object is uniformly *jittered* with respect to the center of the square, such that the circle still resides inside the square. Note that the fraction of the area covered by the objects is given by $\delta = \pi R^2/L^2$.

In Fig. 10 the potential visibility in a jittered scene with $\delta = 0.125$ is shown as a function of distance, for different

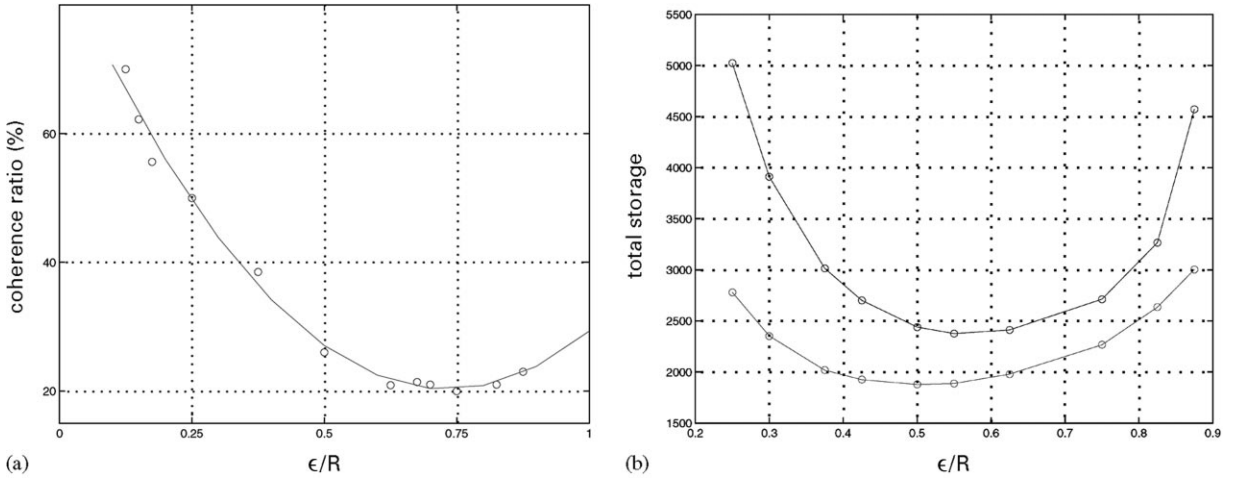


Fig. 9. (a) Average coherence ratio as a function of cell size (b) Total storage size as a function of cell size (in arbitrary units), for the naive data-structure (top), and for the hierarchical data-structure (bottom).

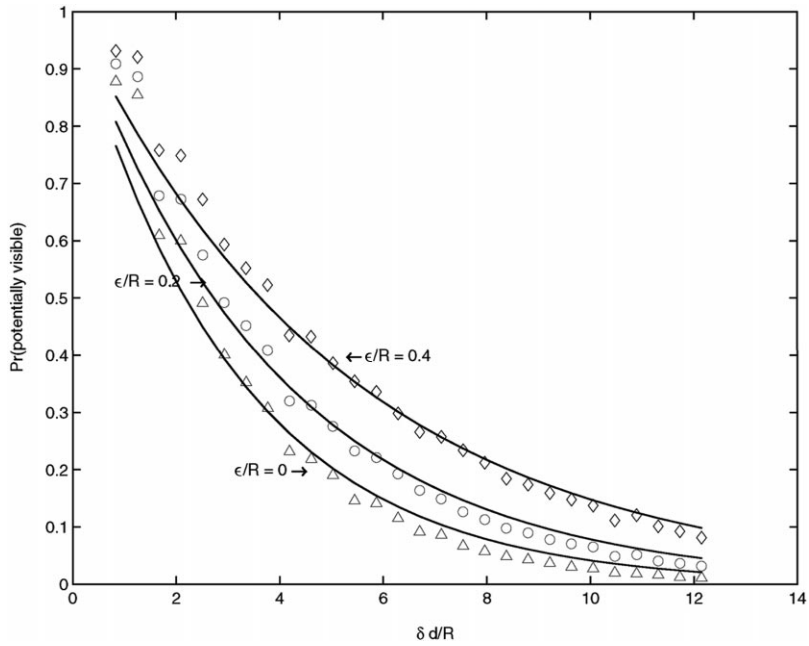


Fig. 10. Potential visibility in a jittered scene, as a function distance, for different viewcell sizes. In this simulation, $L = 5$, and $R = 1$, ($\delta = 0.1257$). Simulation results vs. prediction (3) for a random scene.

viewcell sizes. This is the analogue of the left graph in Fig. 5. These simulation results are compared with the theoretical prediction (3), which was derived for a random scene. The graph shows that except for objects located in the adjacent squares, there is a good agreement between the two.

This agreement can be explained as follows: Recall that an object S is potentially visible if there are no objects inside the region of strong occlusion, Ω_S (Section 2). For long distances, Ω_S intersects with many squares. Let us denote by A_j the intersection area of the j th square that intersects with Ω_S . The probability that the center of the

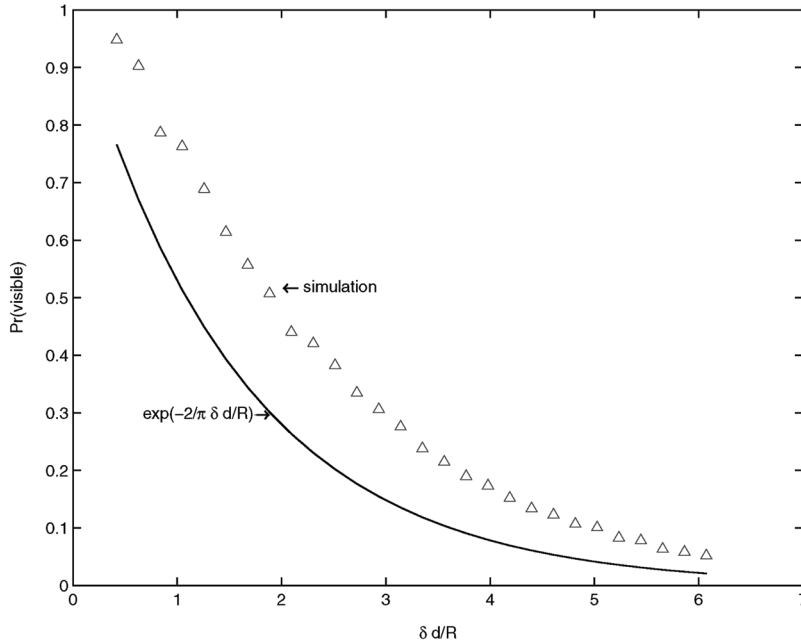


Fig. 11. Visibility probability in a jittered scene with $L = 5$ and $R = 0.5$, ($\delta = 0.0314$), as a function of distance from a point viewcell with $\epsilon = 0$. Average of 100 simulations (triangles), vs. theoretical prediction (5) for a random scene (solid line).

object inside the square does not reside inside A_j is approximately $1 - A_j/L^2$. Thus,

$$\begin{aligned} \Pr(S \text{ potentially visible}) &\approx \prod_j \left(1 - \frac{A_j}{L^2}\right) \approx \prod_j \exp\left(-\frac{A_j}{L^2}\right) \\ &= \exp\left(-\frac{|\Omega_S|}{L^2}\right), \end{aligned}$$

which is exactly the same as in the case of a random scene, (Eq. (3)).

The disagreement between the theoretical prediction for random scenes and the simulation results for a jittered scene is most noticeable for distances of the order of one or two squares. In order to understand this, we note that for example, objects in the neighboring squares are always visible in the jittered scene as there is no other object than can occlude them, which is not necessarily the case for a random scene.

We now turn to the visibility probability. A comparison between the actual visibility in a jittered scene and prediction (5) for a random scene appears in Fig. 11. This is the analogue of the right graph in Fig. 5. As can be seen, visibility decreases exponentially, but at a slower rate than predicted by (5). In order to understand the difference between the two, consider the jittering range (i.e. the maximal deviation of object's center from the center of the square) as an additional parameter. When the jittering range is much larger than the length of the

squares, then the objects locations are approximately random, and visibility approximately follows (5). Clearly, as the jittering range is reduced, on the average more objects become visible. The extreme case when there is no jittering at all (i.e., all objects are centered on a Cartesian grid), achieves the highest visibility. Therefore, our simulations in which the jittering range equals the side of the square, correspond to an intermediate case between randomness and a Cartesian grid.

Since the potential visibility in the jittered scene behaves as (3) the potential visibility set size is approximately given by (8). However, as visibility in the jittered scene decays slower than (5), equation (7) is an underestimate for the actual visibility set size. Therefore, the 'strong occluders' method is even better suited for jittered scenes, as the overhead of the potentially visible set is even lower than (9) for a random scene, as analyzed in the previous section.

Appendix A

A.1. Probability of visibility

To calculate the probability for S to be visible, we first note that regions Ω_1 and Ω_2 have the same area and geometrical shape. Let k_1 and k_2 denote the number of objects in Ω_1 and Ω_2 , respectively. Under our approximation, k_1 and k_2 are independent Poisson distributed

random variables with mean $\rho|\Omega_i|$. Consequently, using (1), we have that

$$\begin{aligned} \Pr(S \text{ visible}) &= \Pr(\text{no objects in } \Omega_S) \\ &\times \sum_{k_1, k_2=0}^{\infty} \Pr(S \text{ visible} | k_1, k_2) \Pr(k_1, k_2) \\ &= e^{-\rho|\Omega_S|} \sum_{k_1, k_2=0}^{\infty} \Pr(S \text{ visible} | k_1, k_2) \\ &\times \frac{e^{-\rho|\Omega_1|} (\rho|\Omega_1|)^{k_1} e^{-\rho|\Omega_2|} (\rho|\Omega_2|)^{k_2}}{k_1! k_2!}. \end{aligned} \quad (\text{A.1})$$

Let $\{y_i^{(1)}\}_{i=1}^{k_1}$ and $\{y_j^{(2)}\}_{j=1}^{k_2}$ denote the y coordinate of the center of the objects in Ω_1 and in Ω_2 , respectively. Under the assumption that there are no excluded volume effects (the fact that circles cannot overlap), $\{y_i^{(1)}\}_{i=1}^{k_1}$ and $\{y_j^{(2)}\}_{j=1}^{k_2}$ are independent identically distributed random variables. Let $F_1(y)$ denote the probability that the y coordinate of the highest point of object i in Ω_1 is below y , i.e.

$$F_1(y) = \Pr(y_i < y - R).$$

Let $f_1(y)$ denote the corresponding probability density function. In a similar manner, let $F_2(y)$ denote the probability that the bottom point of object j in Ω_2 lies above y ,

$$F_2(y) = \Pr(y_j > y + R).$$

If $k_1 = 0$ then $\Pr(S \text{ visible} | 0, k_2) = 1$, regardless of k_2 . Otherwise, when $d \gg R$, the probability that S is visible given $n(\Omega_S) = 0$, $n(\Omega_1) = k_1$ and $n(\Omega_2) = k_2$ is approximately²

$$\Pr(S \text{ visible} | k_1, k_2) \approx$$

$$\Pr\left(\min_{1 \leq i \leq k_2} y_j^{(2)} - \max_{1 \leq i \leq k_1} y_j^{(1)} > 2R\right)$$

which can be evaluated as follows:

$$\begin{aligned} &\Pr\left(\min_{k_2} y_j^{(2)} - \max_{k_1} y_j^{(1)} > 2R\right) \\ &= \int_{-2R}^0 \Pr\left(\max_{k_1} y_i^{(1)} = \xi\right) \Pr\left(\min_{k_2} y_j^{(2)} > \xi + 2R\right) d\xi \\ &= \int_{-R}^R k_1 f_1(y) F_1^{k_1-1}(y) [F_2(y)]^{k_2} dy. \end{aligned} \quad (\text{A.2})$$

Note that (A.2) is also valid in the case $k_2 = 0$, for which $\Pr(S \text{ visible} | k_1, 0) = 1$. Inserting (A.2) into (A.1),

² This approximation slightly underestimates the probability for visibility, since it does not take into account the case when there are no horizontal rays of sight from the viewpoint to the object S but there are diagonal ones. However, when $d \gg R$, these neglected events have a very low probability, and their effect on our approximation is small.

and changing the order of summation and integration yields

$$\begin{aligned} \Pr(S \text{ visible}) &= e^{-\rho(|\Omega_S| + |\Omega_1|)} + e^{-\rho|\Omega|} \int_{-R}^R f_1(y) \rho|\Omega_1| dy \\ &\times \sum_{k_1=1}^{\infty} \frac{(\rho|\Omega_1| F_1(y))^{k_1-1}}{(k_1-1)!} \sum_{k_2=0}^{\infty} \frac{(\rho|\Omega_2| F_2(y))}{k_2!} \\ &= e^{-\rho(|\Omega_S| + |\Omega_1|)} + \rho|\Omega_1| e^{-\rho|\Omega|} \\ &\times \int_{-R}^R \exp(\rho|\Omega_1| F_1(y) \\ &+ \rho|\Omega_2| F_2(y)) f_1(y) dy. \end{aligned} \quad (\text{A.3})$$

We now compute $F_1(y)$ and $F_2(y)$ when $d \gg R$. In this case, Ω_1 and Ω_2 are approximately trapezoids with height d and bases of length $2R$ and 2ϵ and

$$|\Omega_1| = |\Omega_2| = d(R + \epsilon).$$

For each value of y , we calculate the fraction of the area of Ω_1 in which an object center can reside such that its highest point still lies below y . This gives

$$F_1(y) = \begin{cases} \frac{(R+y)^2}{2(R^2 - \epsilon^2)} & \text{for } -R < y < -\epsilon, \\ \frac{1}{2} \left(1 + \frac{2y}{R+\epsilon}\right) & \text{for } -\epsilon < y < \epsilon, \\ 1 - \frac{(R-y)^2}{2(R^2 - \epsilon^2)} & \text{for } \epsilon < y < R. \end{cases}$$

Due to the reflection symmetry in the problem $F_2(y) = F_1(-y)$. We now insert these expressions into (A.3). Noting that $F_1(y) + F_2(y) = 1$ we obtain

$$\Pr(S \text{ visible}) = \left[1 + \rho|\Omega_1| \int_{-R}^R f_1(y) dy\right] e^{-\rho(|\Omega_S| + |\Omega_1|)}.$$

Since $f_1(y) = F_1'(y)$ is a probability density function, its integral equals unity, and (5) follows.

Appendix B

B.1. Visibility set size for a square viewcell

The potential visibility set size for a square viewcell with side 2ϵ is bounded from below and above by (8) with ϵ and $\sqrt{2}\epsilon$, since the square is bounded between two circles with radii ϵ and $\sqrt{2}\epsilon$, respectively. We hence perform a more exact analysis in order to get a sharper estimate. For a square viewcell, and an object at a distance d , the region of strong occlusion Ω_S depends on the angle θ formed between the line connecting the square and the object, and the axis of the square viewcell (Fig. 12). For $d \gg R$, Ω_S is approximately a triangle with

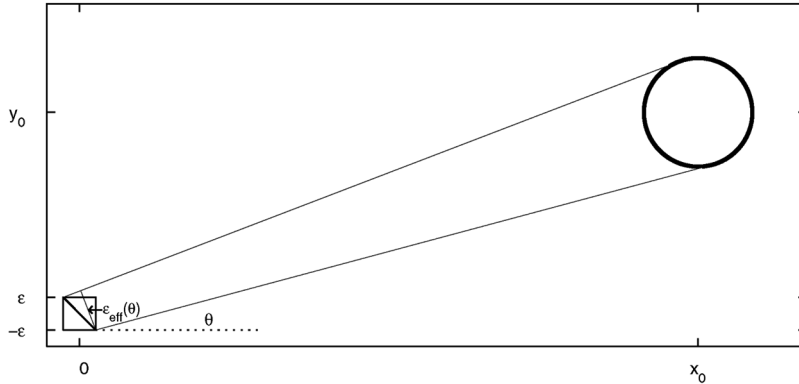


Fig. 12. The effective radius $\epsilon(\theta)$ for an object centered at (x_0, y_0) which forms an angle θ with the square viewcell, for $d \gg R$.

height d and baseline $2(R - \epsilon(\theta))$, where the effective viewcell radius $\epsilon(\theta)$ is given by

$$\epsilon(\theta) = \sqrt{2}\epsilon \sin(\pi/4 + \theta).$$

We divide the plane into 8 sectors, such that in each the angle $\theta \in [0, \pi/4]$. Using (3) with $\epsilon = \epsilon(\theta)$, the average number of potentially visible objects is given by

$$\begin{aligned} N_{\text{potentially visible}} &= 8 \int_0^{\pi/4} d\theta \int_0^\infty dr \frac{\delta}{\pi R^2} r \exp\left(-\frac{2r}{\pi R} \left(1 - \frac{\epsilon(\theta)}{R}\right)\right) \\ &= \frac{8\pi}{\delta} \int_0^{\pi/4} \frac{d\theta}{(1 - (\sqrt{2}\epsilon/R) \sin(\pi/4 + \theta))^2}. \end{aligned}$$

The last integral can be evaluated analytically, though the exact expression is rather complicated. However, a Taylor expansion for $\epsilon/R \ll 1$ yields

$$\begin{aligned} N_{\text{potentially visible}} &\approx \frac{2\pi^2}{\delta} \left(1 + 16 \frac{3 - 2\sqrt{2}}{(2 - \sqrt{2})^2} \frac{\epsilon}{R}\right) \\ &\approx \frac{2\pi^2}{\delta} \frac{1}{(1 - 1.27\epsilon/R)^2}. \end{aligned}$$

Therefore, the effective radius for a square viewcell with side 2ϵ is $\epsilon_{\text{eff}} = 1.27\epsilon$.

References

- [1] Cohen-Or D, Fibich G, Halperin D, Zadicario E. Conservative visibility and strong occlusion for viewspace partitioning of densely occluded scenes, Eurographics '98 pp. 243–53.
- [2] Airey JM, Rohlf HJ, Brooks FP Jr. Towards image realism with interactive update rates in complex virtual building

environments. Computer Graphics (1990 Symposium on Interactive 3D Graphics) 1990;24(2):41–50.

- [3] Hudson T et al. Accelerated occlusion culling using shadow volumes. Proceedings of 13th ACM Symposium on Computational Geometry, Nice, France, June 4–6, 1997.
- [4] Wonka P, Schmalstieg D. Occluder shadows for fast walkthrough of urban environments. EUROGRAPHICS '99, pp. 51–60, September 99.
- [5] Coorg S, Teller S. Temporally coherent conservative visibility. Proceedings of the 12th ACM Symposium on Computational Geometry, 1996.
- [6] Coorg S, Teller S. Real-time occlusion culling for models with large occluders. Proceedings of the 1997 Symposium on Interactive Graphics.
- [7] Sillion F, Drettakis G, Bodelet B. Efficient impostor manipulation for real-time visualization of urban scenery. Proceedings of Eurographics '97, September 1997.
- [8] Funkhouser TA. Database management for interactive display of large architectural models. Graphics Interface '96, May 1996, p. 1–8.
- [9] Cohen-Or D, Zadicario E. Visibility, streaming for network-based walkthroughs. Graphics Interface '98, 1–7, June 1998.
- [10] Chrysanthou Y. Shadow computation for 3D interactive and animation. Ph.D. Thesis, Department of Computer Science, College University of London, January 1996.
- [11] Plantinga H, Dyer R. Visibility, occlusion, and aspect graph. The International Journal of Computer Vision, 1990;5(2):137–160.
- [12] Feller W. An introduction to probability theory and its applications, vol I. New York: Wiley, 1966.
- [13] Hansong Zhang, Dinesh Manocha, Tom Hudson, Kenny Hoff. Visibility culling using hierarchical occlusion maps. Proceedings of ACM SIGGRAPH'97.